

**ORIGINAL RESEARCH**

# PROTOTYPE PORTABLE ELECTRICAL RESISTANCE TOMOGRAPHY

Ahmad Zaenal Hayat\* | Agung Tjahjo Nugroho | Nurul Priyantari

<sup>1</sup>Dept. of Physics, University of Jember,  
Jember, Indonesia

**Correspondence**

\*Ahmad Zaenal Hayat, Dept of Physics,  
University of Jember, Jember, Indonesia.  
Email: zaenalhayat@gmail.com

**Present Address**

Jl. Merpati No. 17, Sampang, 69263,,  
Indonesia

**Abstract**

Tomography is a way to describe something non-destructively. Some types of Tomography are Electrical Resistance Tomography (ERT), Electrical Impedance Tomography (EIT), and Electrical Capacitance Tomography (ECT). This study aims to combine the ECT and ERT systems. The combination uses the ERT technique (Borehole method) and develops until it can be used like ECT. This research conducts three significant stages (design making, designed realization, and examination). The examination is carried out by simulation and experimental measurement. The simulation result is compared to the result of the experimental measurement. The result shows that both have the same patterns, but it has the amplitude of voltage difference pattern. It is because the resistivity result affects the measured voltage difference result. The higher the resistivity result of the medium, the smaller the measured voltage difference.

**KEYWORDS:**

Amplitude, Electrical Capacitance Tomography, Electrical Resistance Tomography, Voltage Different Pattern

## 1 | INTRODUCTION

Tomography comes from the word “Tomo” which means piece<sup>[1]</sup>. Tomography has several types, including Electrical Resistance Tomography (ERT), Electrical Impedance Tomography (EIT), and Electrical Capacitance Tomography (ECT). Some of the types above are types of Tomography from Electrical Tomography (ET)<sup>[2]</sup>. Electrical Impedance Tomography (EIT) is an imaging technique that utilizes the impedance that occurs in a material. A change in this impedance is used to perform imaging<sup>[3]</sup>. Electrical Capacitance Tomography (ECT) is a method to image the inside of a material or in a tube without damaging it by utilizing the dielectric properties in the material or tube<sup>[4]</sup>. Electrical Resistance Tomography (ERT) calculates the resistivity distribution below the surface using voltage and current measurements. Measurements are made using electrodes placed to form a pattern<sup>[5]</sup>.

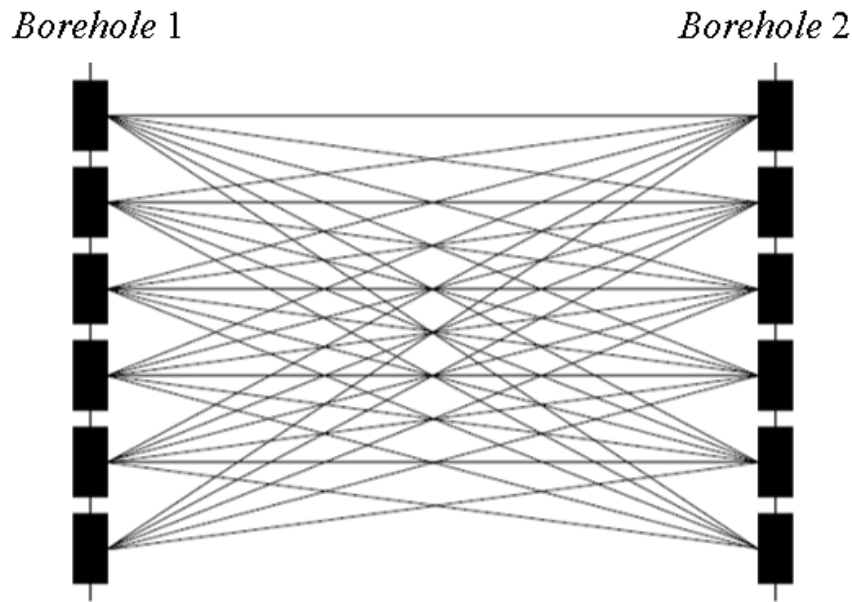


**FIGURE 1** The cross-hole method.

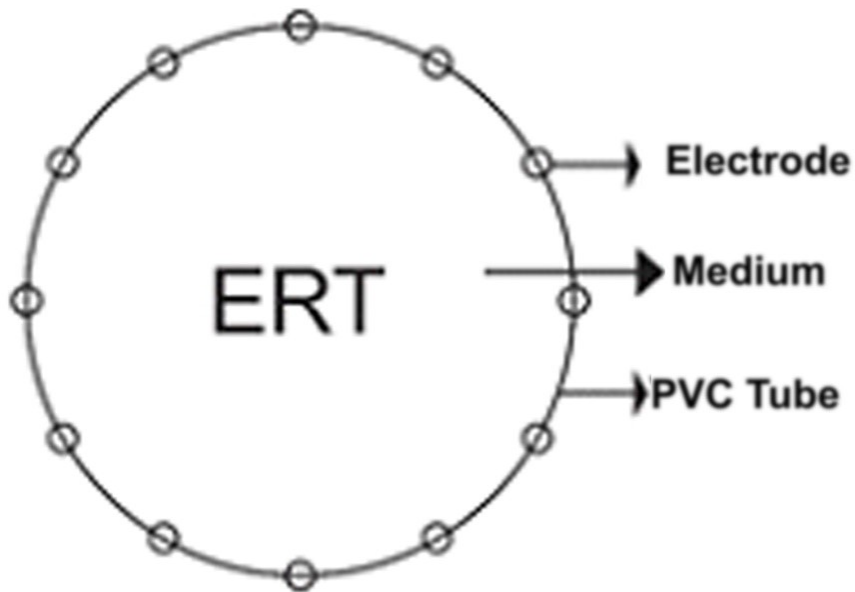


**FIGURE 2** The architectural design.

A study on ERT used on a small scale was conducted by Butler<sup>[6]</sup>. The system used in the study also utilized an electric field, where changes in the electric field would affect changes in the measured voltage difference. In his research, the current and voltage electrodes will be arranged parallel. This method is called the Borehole method<sup>[6-10]</sup>. The Cross-hole method is a tomography method that is carried out using a source electrode (current source point) and potential electrode (measuring point), which are placed under the surface in two horizontally separated boreholes<sup>[11]</sup>. Figure 1 illustrate the cross-hole method.

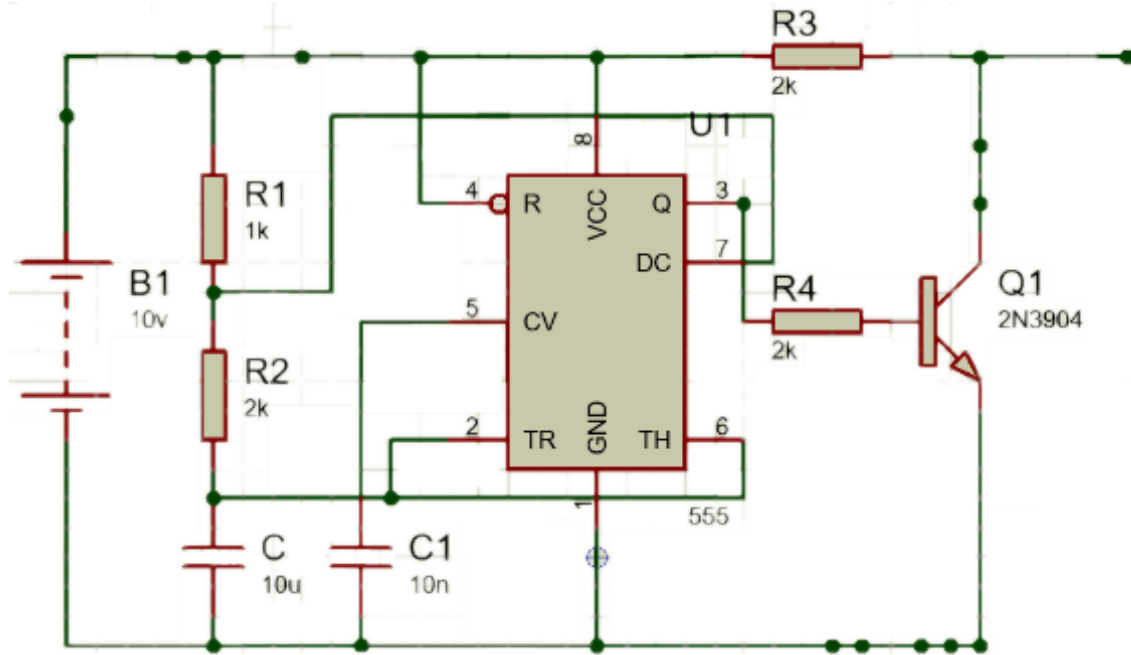


FIGURE 3 The oscillator circuit.

The Cross-hole method is an imaging technique that uses several electrodes in a borehole that can describe the resistivity distribution in the soil. This method can be used with various current-potential electrode arrangements, such as (pole-pole, pole-dipole, dipole-pole, and dipole-dipole) arrangements<sup>[12]</sup>.

## 2 | MATERIAL AND METHOD

The architectural design in this study is a combination of the Borehole and ECT methods, in which the electrodes will surround the surface of the study tube just as in (ECT). Figure 2 shows the ECT architecture.

This study uses electrodes as the input and output media. The electrodes used in this study have a surface area of  $2.5 \text{ mm}^2$ , a length of 5 cm, and are made from copper. The mediums used in this study are sand and water. The use of two types of medium determines the system can run when using mediums with different resistivity values.

This study used voltage as input. The voltage used in this study is 10V. The voltage given is a pulse voltage. The use of pulse voltage is due to minimizing the polarization effect. The polarizing effect occurs because the dipole moments try to align or be in a straight line. This alignment creates a new source<sup>[13]</sup>. The input section uses a Timer circuit driven by the NE555 timer IC. Figure 3 shows the oscillator circuit used in this study.

The measuring instrument used in this study uses an automatic control system. Figure 4 shows the use off Arduino MEGA for the voltage measuring circuit. This system utilizes the Microprocessor as a control center. This system is used so that data retrieval can run quickly. The measurement design in the Figure 5 is performed by measuring the voltage difference between the two electrodes. This voltage difference measurement uses the Rover and Base (RnB) measurement system.

The second step is by moving the rover so that all of the electrodes can function as the rover. The third step is by transferring the base to another electrode. This RnB measurement is continuously carried out until all electrodes function as base and rover.

The data obtained from the measurements will then be analyzed. The analysis method used is the finite difference method. The finite-difference method is a method that utilizes a matrix obtained from a finite-difference grid to show a continuous settlement

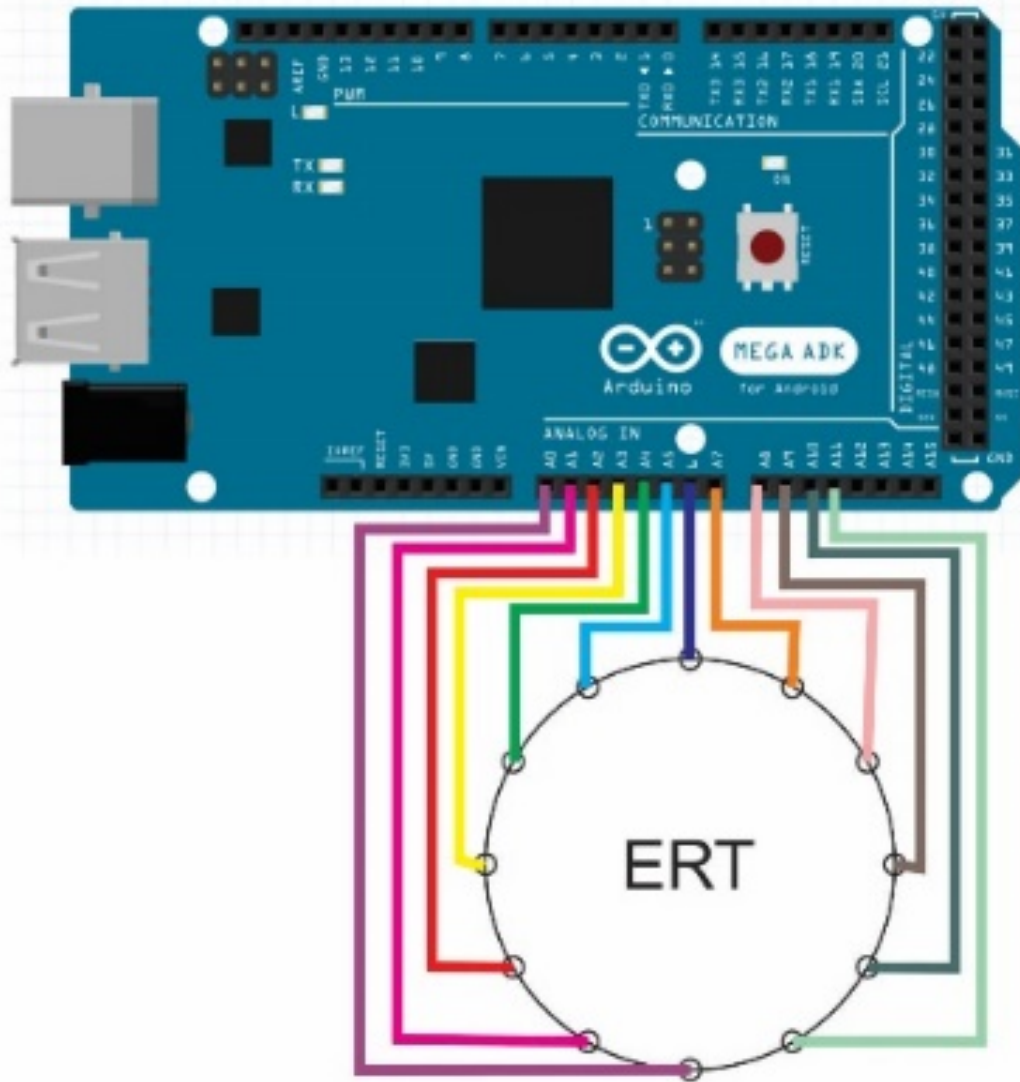


**FIGURE 4** The voltage measuring circuit uses the Arduino MEGA.

domain<sup>[14, 15]</sup>. The finite-difference method uses the partial differential equation (PDE) to solve it. The finite-difference approach equations obtained using the PDE are as follows:

$$\frac{\partial^2 V}{\partial x^2} = \frac{V_{i+1,j} - 2V_{i,j} + V_{i-1,j}}{\Delta x^2} \quad (1)$$

$$\frac{\partial^2 V}{\partial y^2} = \frac{V_{i,j+1} - 2V_{i,j} + V_{i,j-1}}{\Delta y^2} \quad (2)$$

Then the finite-difference approach equation will be obtained as shown in Eq. 3.

$$\nabla^2 V = \frac{V_{i+1,j} - 2V_{i,j} + V_{i-1,j}}{\Delta x^2} + \frac{V_{i,j+1} - 2V_{i,j} + V_{i,j-1}}{\Delta y^2} \quad (3)$$

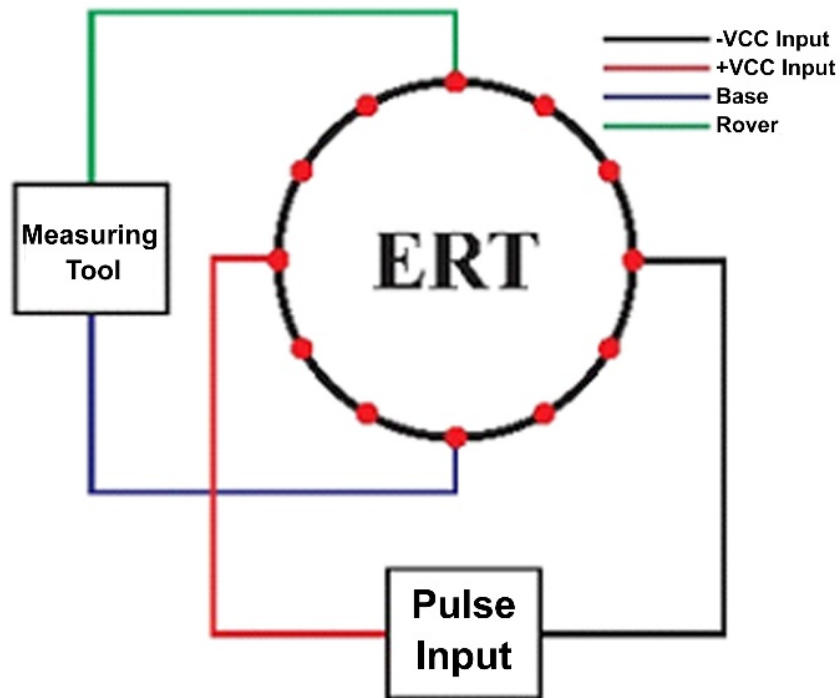


FIGURE 5 The measurement design.



FIGURE 6 The ERT system design top view.



FIGURE 7 The ERT system design side view.

Fitting is performed to make it easier to analyze the data obtained. This study performs fitting using the Fourier series. Fourier series is the breakdown of periodic functions into oscillating functions. Fourier series is widely used in solving differential equations<sup>[16]</sup>. The Fourier series used in this study is as follows:

$$y = \sum_{i=0}^{n=8} a_i \cos(ix\omega) + b_i \sin(ix\omega) \quad (4)$$

Based on Eq. 4, the fitting result is obtained in the 8th Fourier. The fitting result obtained using equation four will then be filtered. The filter is carried out to make it easier to analyze the differences when given different treatments. The filter used in this study

$$\begin{bmatrix} V_{1,1} & \dots & V_{19,1} \\ \vdots & \ddots & \vdots \\ V_{1,19} & \dots & V_{19,19} \end{bmatrix}$$

**FIGURE 8** The matrix 19x19.

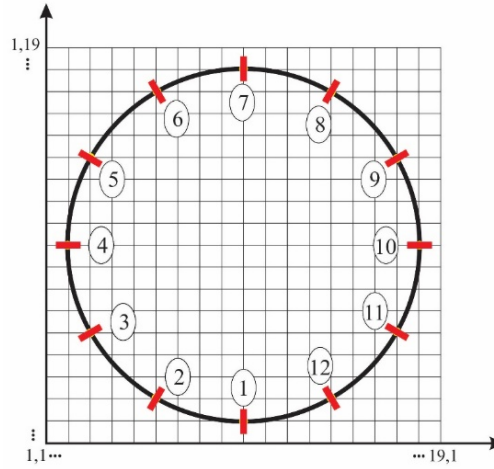


**FIGURE 9** The mapping the research media after being given a grid.

is the LPF (Low Pass Filter). This transformation is carried out to determine the amplitude of each different treatment. This is performed to determine that different patterns of measured voltage differences will have different amplitudes. The transformation used in this study is FFT (Fast Fourier Transform). FFT is an algorithm that can work quickly to complete DFT (Discrete Fourier Transform).

## 2.1 | Result Analysis

## 2.2 | Architectural Design

The architectural design in this study was realized using the basic material of copper cables and Polyvinyl Chloride (PVC) pipe. The copper wire with a cross-sectional area of  $2.5 \text{ mm}^2$  is cut into 12 rods with a length of about 5 cm (see Figure 6). The copper cable functions as an electrode which is then plugged into the PVC pipe. The second material is PVC pipe. PVC pipe parts used are pipe caps, pipe over the shock (pipe joints), and pipe pieces. The three parts are joined and glued together.

Figure 7 points to one electrode, points to two pipe pieces, points to three pipe joints, and points to four-pipe caps. The PVC pipe that is connected is then perforated using a small drill. The drilling results were used to place the prepared copper cables. The copper wire is inserted into a small hole with a copper wire length of about 1 cm in the pipe. The small hole where the copper cable is inserted is then sealed in glue, thereby reducing any leaks.

## 2.3 | Simulation with Finite-Difference Method

In this study, a computational simulation was carried out using artificial data. The results of the simulation will be used to compare the research results. This method makes use of Eq. 3 to get the finite difference method approach. Eq. 5 is the finite different method.

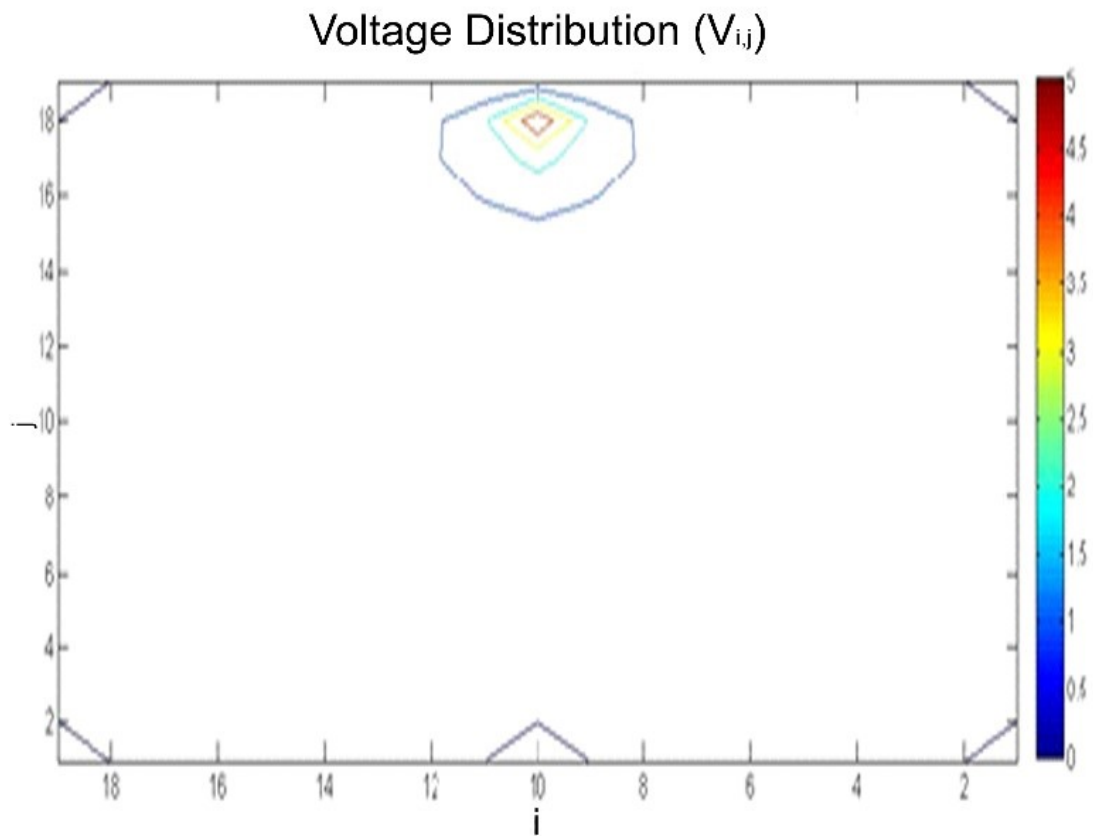
$$V_{i,j} = V_{i+1,j} + V_{i-1,j} + V_{i,j+1} + V_{i,j-1} - 4V_{i,j} \quad (5)$$

The equation (Eq. ref:eg5) was applied to a 19x19 matrix. This matrix was used for research media mapping. Figure 8 shows the matrix used for mapping the research media. Figure 9 shows visualization of mapping the research media after eing given a grid.

Utilizing the matrix and the image above, the 12-point positions were obtained, which corresponds to the electrode position (1). The results obtained in the finite difference method are the voltage distribution. The voltage distribution obtained is visualized as shown in Figure 10.

**TABLE 1** The twelve-point electrode positions.

#	Point	Information
1	$V_{10,2}$	Rover 1, Ground
2	$V_{6,3}$	Rover 2
3	$V_{3,6}$	Rover 3
4	$V_{2,10}$	Rover 4
5	$V_{3,14}$	Rover 5
6	$V_{6,17}$	Rover 6
7	$V_{10,18}$	Rover 7, Input
8	$V_{14,17}$	Rover 8
9	$V_{17,14}$	Rover 9
10	$V_{18,10}$	Rover 10
11	$V_{17,6}$	Rover 11
12	$V_{14,3}$	Rover 12

**FIGURE 10** The voltage distribution simulation uses the finite-difference method.

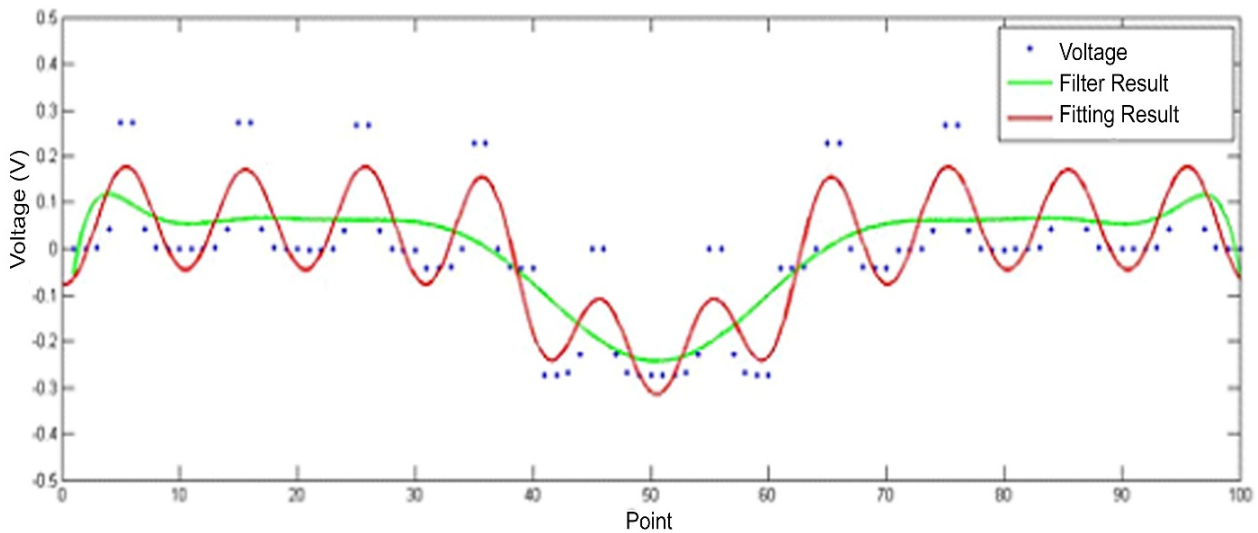
According to Figure 6 , the value of the voltage distribution close to point  $V_{10,18}$  is greater than the value farther away. This is because point  $V_{10,18}$  is the boundary condition point which contains a voltage of 5V. From the results of the voltage distribution simulation, a table of the value of the voltage at the point that corresponds to the position of the electrodes is obtained (Table 2 )

The data obtained from the voltage distribution simulation is fitted to make it easier to analyze the results obtained. Figure 11 show the fitting of the voltage distribution simulation. Fitting is done using the Fourier series. The results obtained after fitting are then filtered. The filter that is done is the Low Pass Filter (LPF). LPF is carried out because the data obtained is in the form of waves with two patterns. LPF is carried out to pass waves with a frequency lower than the cut-off frequency<sup>[17]</sup>. So that data analysis can be carried out more easily.



**TABLE 2** The voltage values according to the position of the matrix.

#	Point	Voltage
1	$V_{10,2}$	0,131
2	$V_{6,3}$	0,178
3	$V_{3,6}$	0,204
4	$V_{2,10}$	0,562
5	$V_{3,14}$	1,012
6	$V_{6,17}$	5,000
7	$V_{10,18}$	1,012
8	$V_{14,17}$	0,562
9	$V_{17,14}$	0,204
10	$V_{18,10}$	0,178
11	$V_{17,6}$	0,131
12	$V_{14,3}$	0,131

**FIGURE 11** The fitting of the voltage distribution simulation uses the finite-difference method.

The results obtained in Figure 11 are then transformed. The transformation is performed using the Fast Fourier Transform (FFT). Figure 12 shows the FFT result after the data has been filtered. FFT is an algorithm that can work quickly to complete DFT (Discrete Fourier Transform)<sup>[18]</sup>. FFT is performed to present data in the frequency domain. This is done to find out any differences that occur at different frequencies. This FFT is done to determine the amplitude in the wave pattern at each different frequency.

Based on Figure 13, the amplitude is different at each frequency. The highest amplitude occurs when the frequency is 1. The amplitude would decrease until it approaches zero as the frequency increases. This proves that the LPF is functioning properly.

## 2.4 | Homogeneous ERT System Measurement Using Water and Sand Medium

According to Figures 13 and Figure 14, the fitting results of the two mediums have almost the same pattern. The difference that occurs in Figure 13 and Figure 14 is the height of the amplitude. The amplitude in the water medium is higher in value than in the sand medium. This proves that the higher the resistivity value of the medium, the lower the amplitude.

## 2.5 | Comparison of Simulations with Experiments in a Homogeneous Manner

Based on Figure 15, it can be seen that there are differences during the simulation and experimentally. The difference is the magnitude of the amplitude that occurs in all three. The difference also occurs during the experiment, in which the amplitude



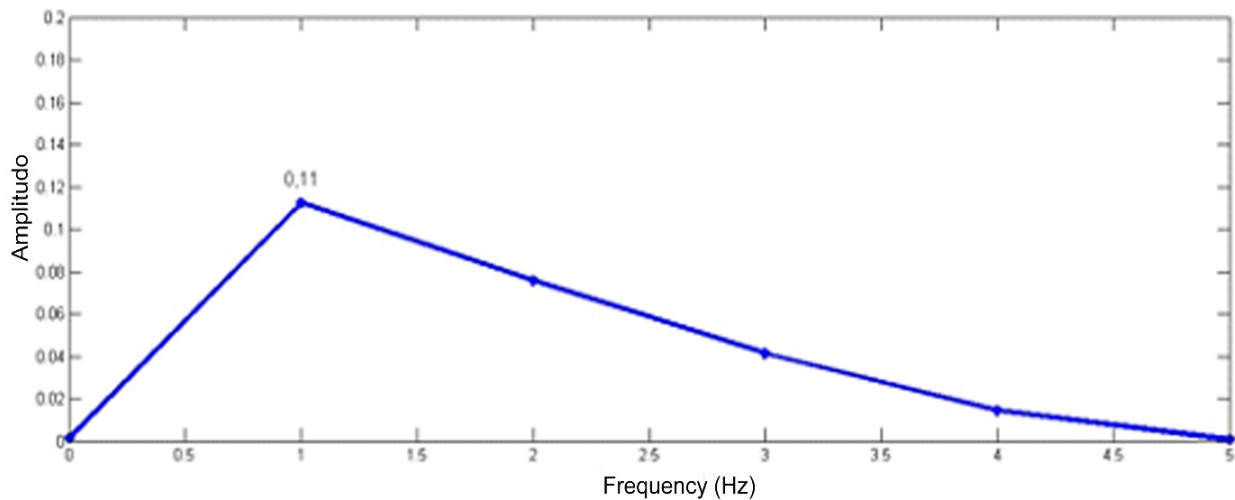


**FIGURE 12** The FFT result after the data has been filtered.

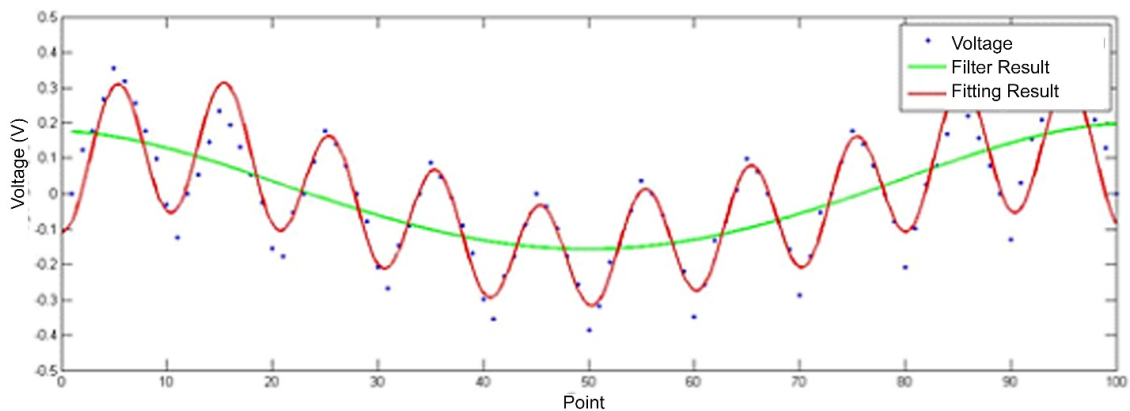


**FIGURE 13** The data fitting result uses water medium..

of the measurement results when using the water medium is greater than when using the sand medium. This is because the resistivity value of water is smaller than sand.

### 3 | CONCLUSION

The conclusion obtained in this study is that the measured voltage difference pattern at each rover is different. The closer the rover is to the input, the greater the voltage difference value. The amplitude of the measured voltage difference pattern obtained when measuring using a water medium is greater than that of the sand medium. This is because the resistivity value of water is smaller than sand.

Further studies that can be carried out to develop this study include reconstructing the data obtained. So that it can be easily analyzed. The second development is to make measurement techniques more real-time. The result is that the measurement can be made in real-time with a visual appearance that is easier to understand

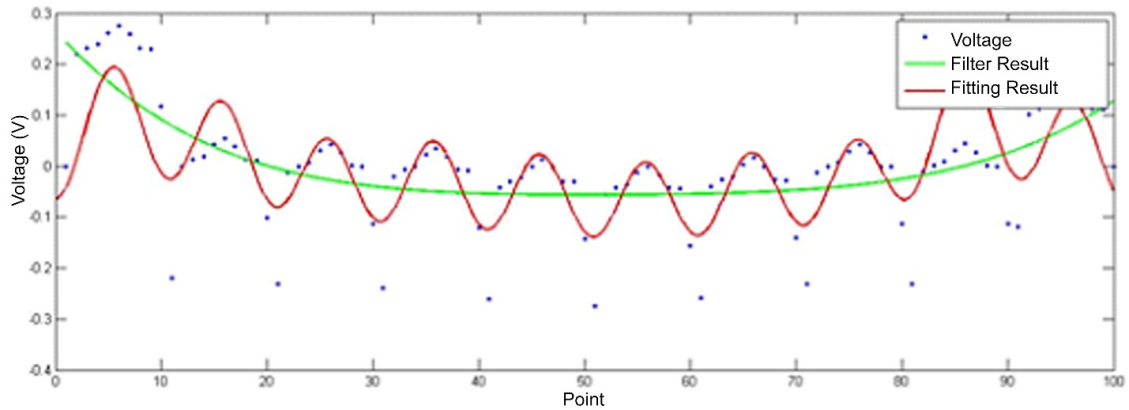


FIGURE 14 the data fitting result uses the sand medium..

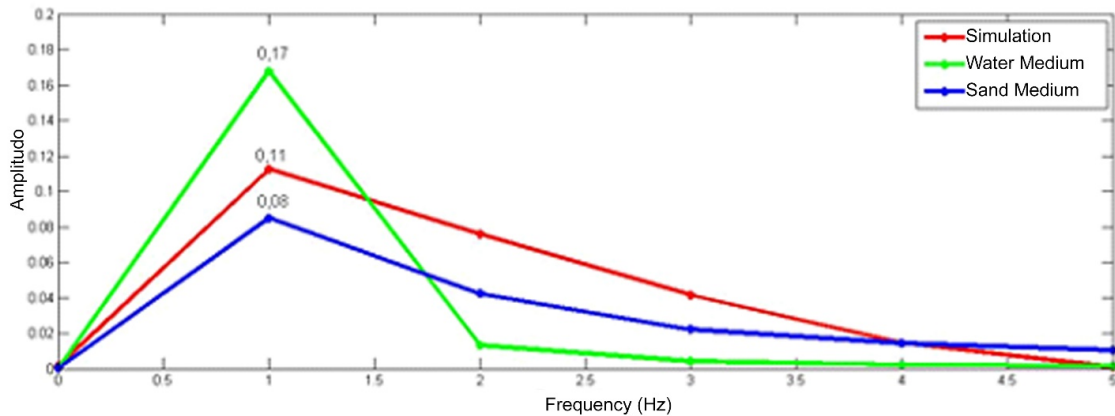


FIGURE 15 The comparison of the results FFT of simulation, water medium, and sand medium.

## CREDIT

**Ahmad Zaenal Hayat:** Methodology, Writing – original draft preparation, Formal analysis, Resource, Acquisition, and Investigation. **Agung Tjahjo Nugroho:** Conceptualization, Supervision, and Writing - reiew and editing. **Nurul Priyantari:** Writing - review and editing, Data Acquisition, Resources.

## References

1. Romans LE. Computed Tomography for Technologists: A Comprehensive Text, second edition,," Computed Tomography for Technologists: A Comprehensive Text. 2 ed. Lippincott Williams & Wilkins; 2018.
2. Ishak S, Rahiman MHF, Salman Sayyidi Siow H, Thiam L, Ali, Mar NA, et al. A review of application electrical resistance tomography for rooted herb tree detection. *Jurnal Teknologi* 2016;78:131–137. [www.jurnalteknologi.utm.my](http://www.jurnalteknologi.utm.my).
3. Harikumar R, Prabu R, Raghavan S. Electrical impedance tomography (EIT) and its medical applications: a review. *Int J Soft Comput Eng* 2013;3:193–198.
4. Masturah MT, Rahiman M, Zakaria Z, Rahim AR, Ayob NM. Design of flexible electrical capacitance tomography sensor. *Jurnal Teknologi* 2015;77:1–3. [www.jurnalteknologi.utm.my](http://www.jurnalteknologi.utm.my).

5. Daily W, Ramirez A, Binley A, LaBrecque D. Electrical Resistance Tomography—Theory and Practice. In: Near-Surface Geophysics Society of Exploration Geophysicists; 2005.p. 525–550.
6. Butler DK. Near-surface Geophysics, vol. 1. Society of Exploration Geophysicists; 2005.
7. Liu LB, Qian RY. Ground Penetrating Radar: A critical tool in near-surface geophysics. *Chinese Journal of Geophysics* 2015;58(8):2606–2617.
8. Everett ME. Theoretical Developments in Electromagnetic Induction Geophysics with Selected Applications in the Near Surface. *Surveys in Geophysics* 2012;33(1):29–63.
9. Carstens G. Near-surface geophysics. *Leading Edge* 2015;34(2):146 – 146.
10. Vanella D, Ramírez-Cuesta JM, Intrigliolo DS, Consoli S. Combining electrical resistivity tomography and satellite images for improving evapotranspiration estimates of citrus orchards. *Remote Sensing* 2019;11(4):373–388.
11. Prabowo RE, Yuliyanto G, Nurwidyanto MI. Pemodelan Tomografi Cross-Hole Metode Geolistrik Resistivitas (Bentuk Anomali Silindris). *Berkala Fisika* 2006;9(1):23–29. [http://eprints.undip.ac.id/1675/1/Pemodelan\\_Tomografi\\_Cross-Hole\\_Metode\\_Geolistrik\\_Resistivitas\\_\(Bentuk\\_Anomali\\_Silindris\).pdf](http://eprints.undip.ac.id/1675/1/Pemodelan_Tomografi_Cross-Hole_Metode_Geolistrik_Resistivitas_(Bentuk_Anomali_Silindris).pdf).
12. Bing Z, Greenhalgh SA. Cross-hole resistivity tomography using different electrode configurations. *Geophysical Prospecting* 2000;45:887–912.
13. Haus HA, Melcher JR. *Electromagnetic Fields and Energy*, vol. 107. Prentice-Hall; 1989.
14. Hartanto AS. Penyelesaian Numerik Persamaan Laplace dan Persamaan Poisson dalam Pelat Persegi Panjang dan Pelat Cakram Dengan Metode Beda-Hingga. PhD thesis, Universitas Sanata Dharma; 2008.
15. Al-Ameen Z, Al-Ameen S, Al-Othman A. Improving the Sharpness of Digital Images Using a Modified Laplacian Sharpening Technique. *IPTEK The Journal for Technology and Science* 2019 jan;29(2):44–48. <https://iptek.its.ac.id/index.php/jts/article/view/3356>.
16. Hammad AI, Khalil R. Fractional fourier series with applications. *American Journal of Computational and Applied Mathematics* 2014;4(6):187–191. <http://journal.sapub.org/ajcam>.
17. Winder S. *Analog and Digital Filter Design*. 2 ed. Elsevier Science; 2002.
18. Brigham EO. *The Fast Fourier Transform and Its Applications*. 2 ed. Prentice-Hall; 1988.

**How to cite this article:** Hayat A.Z., Nugroho A.T., Priyantari N. (2021), Prototype Portable Electrical Resistance Tomography, *IPTEK The Journal of Technology and Science*, 32(3):136-146.